

Article

# The influence of the angstrom-scale roughness on the laser-induced damage threshold of the ZnGeP<sub>2</sub> single crystal

Nikolai Yudin<sup>1,2,3\*</sup>, Andrey Khudoley<sup>4</sup>, Mikhail Zinoviev<sup>1,2,3</sup>, Sergey Podzvalov<sup>1,3</sup>, Elena Slyunko<sup>1,3</sup>, Elena Zhuravleva<sup>1</sup>, Maksim Kulesh<sup>1</sup>, Gennadij Gorodkin<sup>4</sup>, Pavel Kumeisha<sup>4</sup> and Oleg Antipov<sup>5</sup>

- <sup>1</sup> National Research Tomsk State University, Tomsk 634050, Russia; rach3@yandex.ru (N.Y.); muxa9229@gmail.com (M.Z.); cginen@yandex.ru (S.P.); elenohka266@mail.ru (Y.S.); lenazhura@mail.ru (Y.Z.); kyleschMM2000@yandex.ru (M.K.);
- <sup>2</sup> V.E. Zuev Institute of Atmospheric Optics SB RAS, Tomsk, 634055 Russia; rach3@yandex.ru (N.Y.); muxa9229@gmail.com (M.Z.);
- <sup>3</sup> LOC LLC, Tomsk, 634050, Russia; rach3@yandex.ru (N.Y.); muxa9229@gmail.com (M.Z.); cginen@yandex.ru (S.P.); elenohka266@mail.ru (Y.S.);
- <sup>4</sup> A.V. Luikov Heat and Mass Transfer Institute NASB, Minsk, 220072, Belarus; khudoley@hmti.ac.by (A.K.); gorodkin@hmti.ac.by (G. G.); pavel.k@hmti.ac.by (P.K.);
- <sup>5</sup> Institute of Applied Physics of the Russian Academy of Sciences, 46 Ulyanov St., Nizhny Novgorod, 603950 Russia; antipov@ipfran.ru (O.A.);
- \* Correspondence: [rach3@yandex.ru](mailto:rach3@yandex.ru) (N.Y.); Tel.: +7-996-938-71-32.

**Abstract:** Magnetorheological processing was applied to polish the working surfaces of the ZnGeP<sub>2</sub> single crystal, in which a non-aqueous liquid with magnetic particles of carbonyl iron with the addition of nanodiamonds was used. Samples of a single crystal ZnGeP<sub>2</sub> with an angstrom level of surface roughness were received. The use of MRP has allowed more accurately characterizing possible structural defects that have emerged on the surface of a single crystal and have a size of ~ 0.5-1.5 μm. The LIDT value at the indicated orders of magnitude of the surface roughness parameters is determined not by the quality of polishing, but by the number of point depressions caused by physical limitations of the structural configuration of the crystal volume. These results are in good agreement with the assumption made about a significant effect of the concentration of dislocations in a ZnGeP<sub>2</sub> crystal on LIDT.

**Keywords:** Laser induces damage threshold; ZnGeP<sub>2</sub>; Magnetorheological polish

## 1. Introduction

Repetitively pulsed coherent powerful radiation sources of mid-IR range have a wide variety of applications in many areas, such as: material processing (glass, ceramics, or semiconductors) [1,2]; medicine, including disease diagnosis using gas analysis and resonance ablation of biological tissues [4]. Coherent radiation sources capable of generating powerful pulsed radiation in the wavelength range of 3.5-5 μm are relevant when creating lidar systems based on the differential absorption method for the control of greenhouse gas emissions (since the most intensive absorption lines of greenhouse gases are in this spectral ranges) [4-6]. One of the most effective solid sources of coherent radiation in the mid-IR range are optical parametric oscillators (OPO).

Currently, the most powerful OPOs in the wavelength range of 3.5-5 μm are developed based on nonlinear-optical ZnGeP<sub>2</sub> (ZGP) crystals [7]. The OPO data can generate radiation with an average power up to 160 W or pulse energy up to 200 mJ with the pulse duration of 20...60 ns and the repetition rate from the Hz units up to 100 kHz [8-10]. However, long-term work without failure of powerful OPOs based on ZGP is limited to the laser-induced damage threshold (LIDT) of the surface of the given material. In this regard, the potential for the practical use of the OPO data of the mid-IR range is associated with the need to improve the methods for processing of the working surfaces of crystals to

increase their LIDT. The problem of ZGP optical breakdown by laser radiation at wavelengths from 1.064  $\mu\text{m}$  to 10  $\mu\text{m}$  is devoted to several published earlier articles [11-18]. These articles have revealed a significant difference in the magnitude of the LIDT of the ZGP crystal at the wavelengths of 1.064  $\mu\text{m}$  and 2.1  $\mu\text{m}$  [11]. The dynamic visualization of the breakdown process with laser radiation at a wavelength of 2.1  $\mu\text{m}$  in the volume of ZGP showed that an avalanche-shaped temperature increase occurs within the nonlinear-optical element [12]. An increase in the ZGP breakdown threshold with a decrease in the duration of the pump radiation pulses is "indicated in favor of the thermal nature of the breakdown for nanosecond pulses due to abnormal infrared absorption." In [14], it was shown that cooling of a crystal to temperature of  $-60^{\circ}\text{C}$  leads to an increase in the LIDT by 1.5-3 times up to 9  $\text{J}/\text{cm}^2$  at the wavelength of the acting laser radiation of 2.091  $\mu\text{m}$  and the frequency of 10 kHz pulses.

In [15] it was reported that the LIDT of ZGP elements at a wavelength of 9.55  $\mu\text{m}$  was determined by the intensity of the acting beam of 142  $\text{MW}/\text{cm}^2$  with the pulse duration of 85 ns and the repetition rate of 1 Hz, which is  $\sim 9.5 \text{ J}/\text{cm}^2$  in terms of energy density pulses. In the articles it was also reported, in particular, that the laser damage threshold of the ZGP surface is limited rather by the level of the power density of pump radiation, but not by the radiation intensity [16]. The direct dependence of LIDT on the growth technology and optical quality of crystals is demonstrated in [14].

In [17, 18], it was shown that improving the polishing of ZGP working surfaces and a decrease or complete removal of the near-surface fractured layer leads to an increase in the breakdown threshold. In [17], it was shown that a decrease in the near-surface fractured layer led to a decrease in  $R_q$  by two times, a change in the PV parameter was more than 5 times, the LIDT in regard to energy density increased by 2 times. LIDT at a wavelength of 2.05  $\mu\text{m}$  and the pulse frequency of 10 kHz for ZGP samples with a sputtered antireflection coating was improved from 1  $\text{J}/\text{cm}^2$  to 2  $\text{J}/\text{cm}^2$ . An increase in LIDT was achieved by improving polishing of the surface of ZGP samples. At the same time, the results of the studies presented in [14] show that an almost unchanged polishing parameter  $R_z$  and varying the  $R_q$  parameter by more than four times as well as varying the  $R_a$  parameter by more than 5 times did not lead to any changes in LIDT. It was put forward to the assumption that it was the irregularities of the polished surface (peaks and depressions) described by the  $R_z$  parameter contribute to the optical breakdown mechanism and can be "seed" inhomogeneities to initialize the optical breakdown due to field effects at a wavelength of 2.091  $\mu\text{m}$ .

Thus, previous studies indicate that the quality of the polishing of the ZGP surface significantly affects the LIDT value, which in turn limits the reliability of coherent mid-IR radiation sources produced based on a nonlinear ZGP crystal. These circumstances stimulate the development of new polishing methods that provide better surface roughness and a higher LIDT value.

One of the promising methods for improving the surface quality is magnetorheological polishing [19], which, among other things, is increasingly used in processing of laser crystals to increase the radiation resistance threshold and reduce the roughness level. The research presented in this article is devoted to checking the possibility of using magnetorheological processing as a method for removing a defect layer after fine polishing and reducing the level of surface roughness of a ZGP single crystal. The influence of magnetorheological processing on the LIDT of ZGP was estimated.

## 2. Samples under study and their parameters

Two samples of a ZGP single crystal were used for research: sample No. 1 and No. 2 with dimensions of  $6 \times 6 \times 20 \text{ mm}^3$ . The samples under study were cut from a single-crystal ZGP boule (manufactured by LLC "LOK", Russian Federation) at angles  $\theta = 54.5^{\circ}$  and  $\varphi = 0^{\circ}$  relative to the optical axis. A single crystal  $\text{ZnGeP}_2$  boule was grown using the Bridgman method in the vertical direction on an oriented seed; the growth was carried out from a molten polycrystalline compound previously synthesized using the two-temperature

method [20]. The radiation absorption, taking into account multiple reflections from the crystal faces, at a wavelength of 2.097  $\mu\text{m}$  for both samples was 0.03  $\text{cm}^{-1}$ .

The phase composition of the samples under study was determined prior to the study using X-ray diffraction analysis. According to the result of X-ray structural analysis, no foreign phases were detected in all the samples under study (Table 1).

**Table 1.** Results of X-ray diffraction analysis of the samples under study

Sample	Detected phases	Phase content, mass %	Lattice parameters, $\text{\AA}$
Sample №1	ZnGeP <sub>2</sub>	100	$a = 5.4706$ $c = 10.7054$
Sample №2	ZnGeP <sub>2</sub>	100	$a = 5.4707$ $c = 10.7056$

Holograms of the internal volume of the samples under study were obtained using a digital holographic camera DHC-1.064, manufactured by LLC "LOK". Reconstruction of the produced digital holograms was carried out to characterize volumetric defects. The limiting resolution of the method was 3  $\mu\text{m}$  (a detailed description of the digital holography technique, including those applied to visualization of defects in ZGP and a description of the holographic camera used, is given in [21]). No volume defects with linear dimensions  $\geq$  of limiting resolution of the applied holographic method were detected in all three samples used in this work.

The initial polishing of the working surfaces of both test samples was carried out on a 4-PD-200 polishing and finishing machine (SZOS, Republic of Belarus). The initial processing of the working surfaces of all samples consisted of polishing on a cambric polishing pad using ACM 0.5/0 synthetic diamond powder (average grain size of 270 nm). The removal of the material was  $\sim 50 \mu\text{m}$ , which allowed removing the fractured layer formed in the process of cutting the crystal into oriented plates and their preliminary grinding. Then the samples were additionally polished on a cambric polishing pad using ACM 0.25/0 synthetic diamond powder. After that, the samples were polished on a resin polishing pad made of polishing resin using ACM 0.25/0 synthetic diamond powder.

Working surfaces of sample No. 2 were additionally subjected to magnetorheological processing (MRP) from two ends. MRP was carried out on a 5-axis CNC machine UMO-00.00.000 (ITMO, Republic of Belarus). For MPO, a non-aqueous liquid with magnetic particles of carbonyl iron and nanodiamonds was used. A two-stage MRP was used to increase the productivity of material removal from the surface, which included hard and soft modes, differing in the size of the gap between the impeller and the workpiece. A ZGP crystal sample was fixed on the installation using a holder made of fluoroplastic.

The surface roughness of samples 1 and 2 was measured on a 3D optical profilometer MicroXAM-800 (KLA-Tencor, USA). Sample 2 was measured twice before and after MRP. A PSI phase mode and a Nikon X50 lens were used for all samples. The field of view was 116x152  $\mu\text{m}$ . The following parameters were assessed in accordance with ISO 4287-2014: the root-mean-square roughness depth ( $R_q$ ), the arithmetic mean deviation of the roughness profile from the midline ( $R_a$ ) and the sum of the average absolute values of the heights of the five largest profile protrusions and the depths of the five largest profile valleys ( $R_z$ ).

The material loss from the surface after MRP was estimated using the gravimetric method, for which a Pioneer PA214C analytical balance (Ohaus, Switzerland) with a measurement resolution of 0.0001 grams was used. The density taken in calculations of material loss from the surface is 4.16  $\text{g}/\text{cm}^3$ .

### 3. Setup parameters and technique for determining the LIDT threshold of the samples under study

A Ho:YAG laser generating radiation at a wavelength of 2.097  $\mu\text{m}$  pumped by a continuous thulium fiber laser was the source of radiation. The Ho:YAG laser operated in the active Q-switched mode with a pulse duration  $\tau=35$  ns and a pulse repetition rate of 10 kHz. The measured diameter in all experiments was  $d=350\pm 10$   $\mu\text{m}$  at the e-2 level of the maximum intensity. The maximum average radiation power generated by the Ho:YAG laser was 20 W in a linearly polarized Gaussian beam (parameter  $M2 \leq 1.2$ ).

The schematic layout of the experimental stand is shown in Fig. 6. The power of the incident laser radiation was changed using an attenuator consisting of a half-wave plate ( $\lambda/2$ ) and a polarizing mirror (M1). A Faraday isolator (F.I.) was used to prevent the reflected radiation from entering the laser, which prevented an uncontrolled change in the parameters of the incident radiation. The average laser power ( $P_{av}$ ) was measured before each experiment with an Ophir power meter (P.M.).

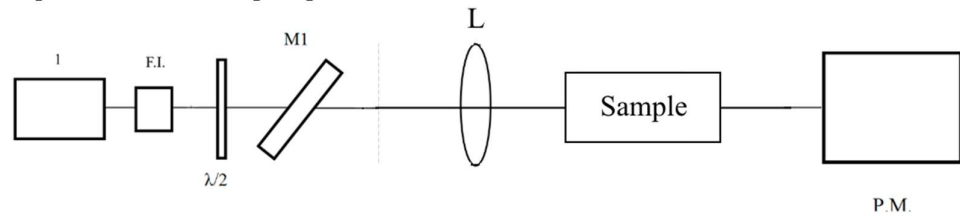


**Figure 1.** Optical schematic layout of the experimental setup: 1 is the Ho:YAG laser, F.I. is the Faraday isolator,  $\lambda/2$  is the half-wave plate, M1 is the polarizing mirror, L is the lens, P.M. is the Ophir power meter

According to the international standard ISO11146 [22], the effective area of a Gaussian beam is determined as  $S = \pi d^2/4$  [22]. The energy density of laser radiation was determined by the formula:

$$W = 8 P_{av}/(f\pi d^2), \quad (1)$$

The energy density of laser irradiation was determined by the formula (2)

$$P = 8 P_{av}/(f \tau \pi d^2) \quad (2)$$

where  $d$  is the diameter of the laser beam,  $f$  is the pulse repetition rate,  $\tau$  is the duration of laser pulses.

The "R-on-1" technique was used to determine the LIDT of the samples, which requires less space on the sample surface as compared to the "S-on-1" technique and, therefore, can be used for samples with a limited aperture, however, it is considered coarser [23]. The essence of this technique is that each individual region of the crystal is irradiated with laser radiation with a sequential increase in the intensity of the laser radiation until an optical breakdown occurs or a predetermined value of the energy density is reached. In our work, the study was carried out with an exposure duration  $\tau_{ex}=5$  s. The sample under study was exposed to packets of laser pulses with a fixed energy density level, which did not cause damage to the crystal surface. Then, the energy density level was increased with a step of  $\sim 0.1$  J/cm<sup>2</sup>. The experiment was terminated when a visible damage appeared on one of the surfaces of the nonlinear element. Then, the sample was moved 0.5 mm in height or width using a two-dimensional movement; the experiment was repeated 5 times. The optical breakdown probability was obtained by plotting the cumulative probability versus the optical breakdown energy density. The value of the LIDT ( $W_{0d}$ ) was taken to be the energy density corresponding to the approximation of the optical breakdown probability to zero. Fig. 7 shows the results of measuring the LIDT using the R-on-1 technique. In the presented plots, the ordinate represents the probability of optical breakdown in relative units, normalized to unity, and the abscissa represents the energy density of the testing laser radiation.

The average value of the threshold energy density  $W_{av}$  and the mean square error of its determination  $\langle \Delta W_{av}^2 \rangle$  were calculated for each series of measurements after which an optical breakdown was observed, using the following formulas

$$W_{av} = \frac{\sum W_i n_i}{N} , \quad (3)$$

$$\langle \Delta W_{av}^2 \rangle = \frac{\sum (\langle W_{av} \rangle - W_i)^2 n_i}{N(N-1)} , \quad (4)$$

where N is the total number of damaged areas,  $W_i$  is the threshold energy density in one of the irradiated regions,  $n_i$  is the number of regions with a breakdown threshold  $W_i$ .

To find the confidence interval of the LIDT value ( $W_D$ )

$$W_D = W_{av} \pm k \langle \Delta W_{av}^2 \rangle^{1/2} , \quad (5)$$

where k is the Student's coefficient, the Student's t-distribution was used for the confidence probability [24,25]

$$F(k, N) = \frac{\Gamma(N/2)}{\sqrt{\pi(N-1)}\Gamma[(N-1)/2]} \int_{-k}^k \left(1 + \frac{z^2}{N-1}\right)^{-N/2} dz , \quad (6)$$

where  $\Gamma$  is the gamma function.

After the absorption of the samples was determined, the values of the LIDT were obtained in terms of the energy density -  $W_{od}^E$  and the power density -  $W_{od}^P$  of the testing laser radiation at the probability  $P_D = 0$  for each sample, according to the method described above. The average value of the energy density -  $W_{av}^E$  and the power density -  $W_{av}^P$  of the testing radiation, at which the optical breakdown of the sample occurred, was calculated using formulas (1), (2), (3) - (6), and the confidence interval of the LIDT the values in terms of energy density -  $W_D^E$  and power density -  $W_D^P$  at a confidence level of 0.98 was determined. The experimental results are presented in Table 3.

#### 4. Experimental results and their discussion

The results of measuring the roughness parameters of the samples are presented in Table 2.

**Table 2.** Surface roughness parameters of samples

Roughness parameters	Sample 1	Sample 2	
		initial	after MRP
$R_z$ , nm	1,56	1,46	1,06
$R_a$ , nm	0,227	0,218	0,154
$R_q$ , nm	0,289	0,274	0,193

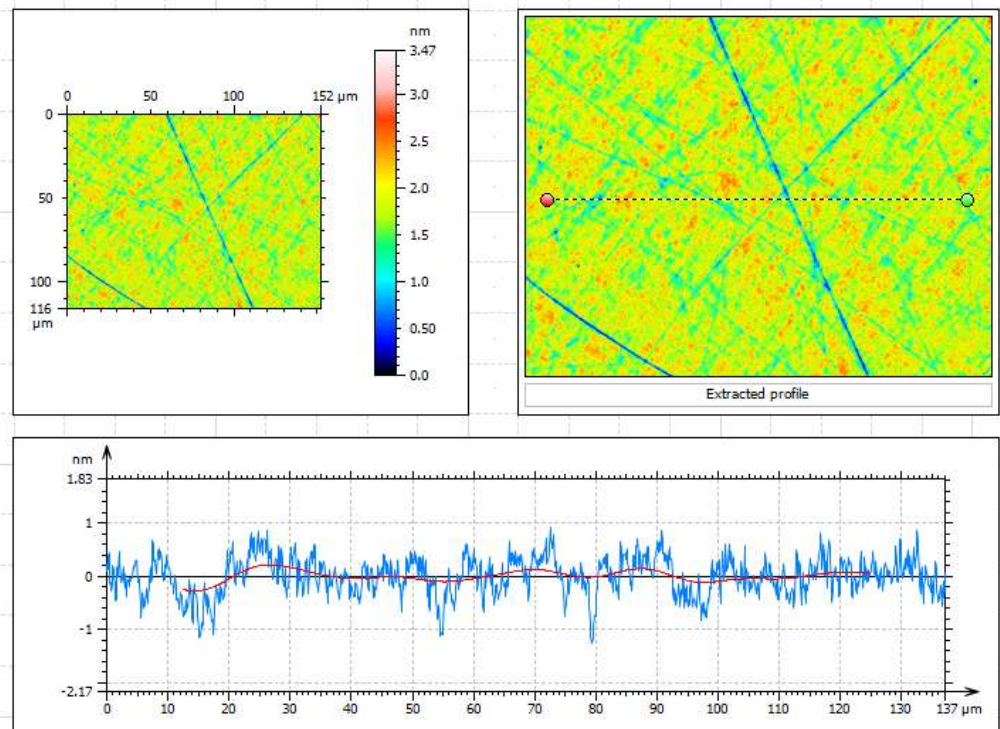


Figure 2. Surface topography and roughness profile of sample No. 1

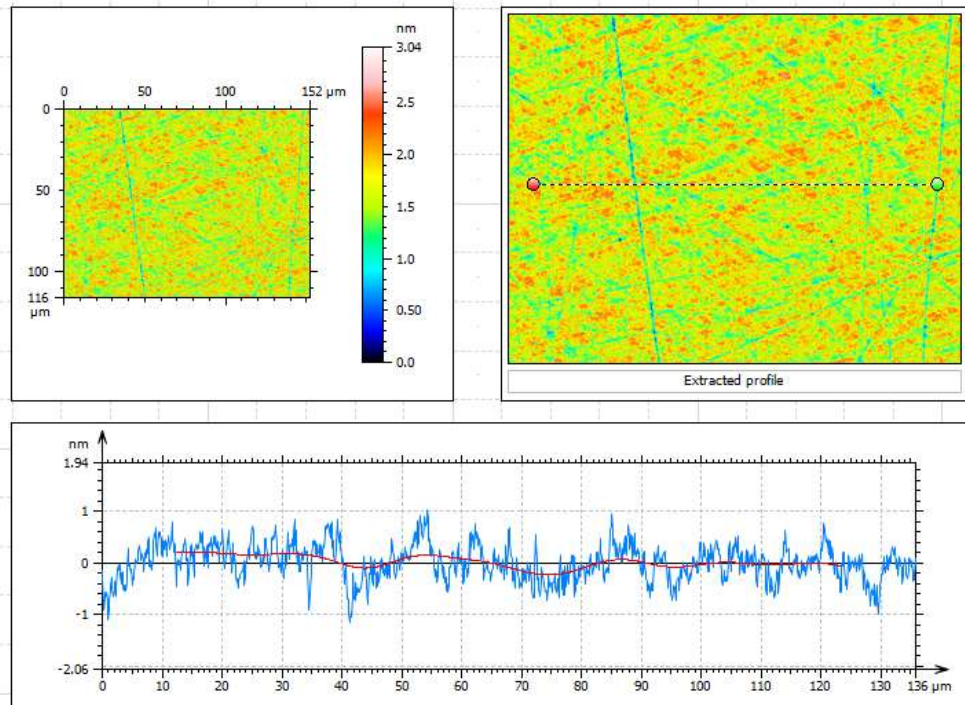
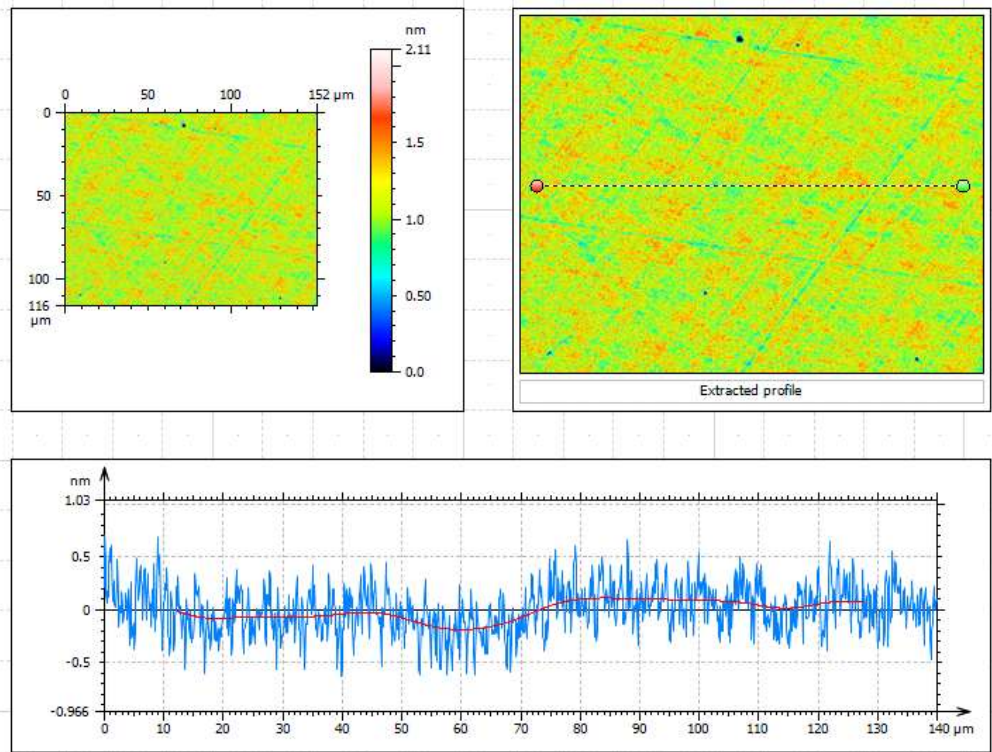


Figure 3. Surface topography and roughness profile of sample No. 2, before MRP



**Figure 4.** Surface topography and roughness profile of sample No. 2 after MRP

The analysis of the surface topography of sample No. 1 and sample No. 2 polished using conventional technology showed that the surface relief was formed under the influence of multidirectional movement of the working tool, there are single extended scratches up to 1.3 nm deep. The surface topography of sample 2 after MRP does not contain the indicated scratches and is represented by a less textured profile formed under the influence of a magnetorheological fluid. A significant improvement in roughness parameters by 1.37-1.42 times is observed near the surface after MRP. In contrast to [17, 18], where the authors reached the nanometer and subnanometer level of the surface roughness of the ZGP crystal samples, the samples studied in this article had an angstrom roughness level:  $R_a$  2.27 Å for sample No. 1 and  $R_a$  1.54 Å for sample No. 2 after MRP.

All surfaces have single point depressions, most likely due to imperfection of the internal structure of the crystal. These defects are hardly noticeable after traditional polishing because they are partially or completely erased. After MRP, the material is removed from the surface practically without any damage, which more clearly visualizes the areola of the defect and makes allows establishing the true size of the point structural imperfection - 0.5-1.5 microns.

The removal of the material after MRP from the surfaces of sample 2 was as follows: side A was 6.95 μm, side B was 9.50 μm. In fact, the area of 22x20 mm instead of 6x6 mm was treated after MRP. Therefore, the total processing time for side A was 435 minutes, and for side B it was 345 minutes. If we subtract the time associated with the acceleration and reversal of the working tool from the total MPO time, then the effective time spent on the working tool on the crystal surface was 8.2% of the total time: for side A it was 28 minutes, for side B it was 36 minutes. In this regard, it is advisable in the future to provide a group type of crystal processing during MRP to increase the efficiency of the use of equipment.

Fig. 5, Fig. 6. and Table 3 show the results of the LIDT study of sample No. 1 (polished using conventional technology) and sample No. 2 immediately after MRP polishing.

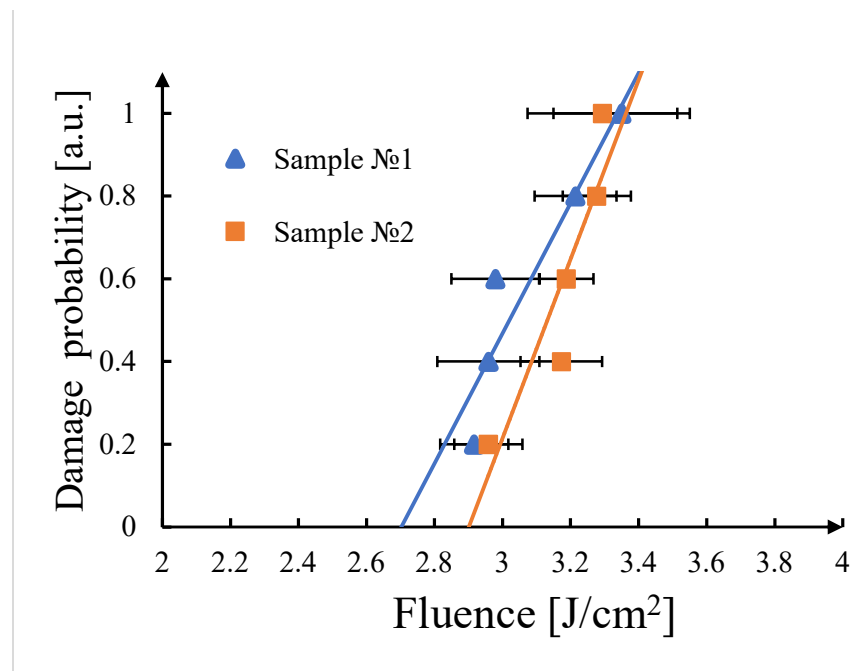


**Figure 5.** Dependence of the optical breakdown probability of samples No. 1 (▲) and No. 2 (■) on the energy density of the incident laser radiation

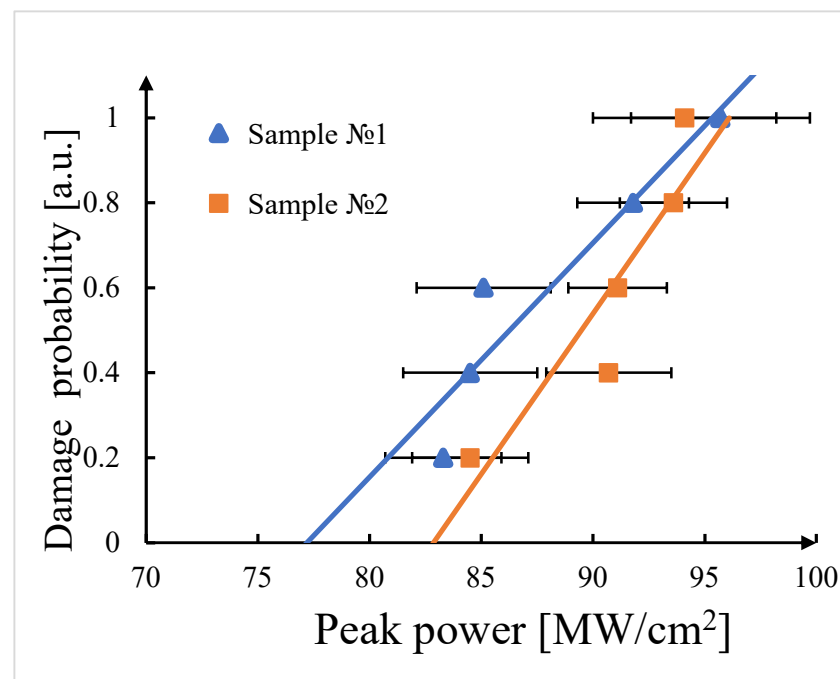


**Figure 6.** Dependence of the optical breakdown probability of samples No. 1 (▲) and No. 2 (■) on the power density of the incident laser radiation

**Table 3.** The results of determining the LIDT of the studied ZGP samples. The values of the energy density  $W_{od}^E$  and the power density  $W_{od}^P$  with a probability of the optical breakdown of 0, the average value of the energy density  $W_D^E$  and the power density  $W_D^P$ , considering the measurement error, Student's coefficient - k with a confidence probability of 0.98, the number of measurements is N

sample	N	f,	$\tau$ ,	k	$W_D^E$ , J/cm <sup>2</sup>	$W_{0d}^E$ , J/cm <sup>2</sup>	$W_D^P$ ,	$W_{0d}^P$ ,
		kHz	ns		( $\lambda$ -2,097 MKM)	( $\lambda$ -2,097 MKM)	MW/cm <sup>2</sup>	MW/cm <sup>2</sup>
						( $\lambda$ -2,097 MKM)	( $\lambda$ -2,097 MKM)	
№1	5	50	35	3,7	(3,1±0,3)	2,7	(88±9)	77
№2	5	50	35	3,7	(3,2±0,2)	2,9	(91±6)	83

As can be seen from the results of determining LIDT (Fig. 5, Fig. 6, and Table 3), the difference in the LIDT in the energy density and the power density for two samples fits into the error of the LIDT determination technique, even though a significant improvement in roughness parameters by 1.37-1.42 times is observed on the surfaces of sample No. 2 after MRP. At first, the results obtained contradict the data [17, 18] where an improvement in roughness parameters by 2.1 times led to an increase in LIDT by 1.6 times. However, it should be noted that in [17] the  $R_z$  parameter was reduced from 225 nm to 41 nm, and the  $R_q$  parameter from 1.2 nm to 0.57 nm (the minimum achieved value of the  $R_z$  parameter was an order of magnitude larger than the dimension of the parameters of the ZGP crystalline lattice). Based on the results presented in Table 2, both polishing techniques presented in this article have allowed obtaining a surface with roughness (estimated by the parameters  $R_a$ ,  $R_q$ , and  $R_z$ ) of the same order of dimension with the parameters of the unit cell of the ZGP crystalline lattice ( $a=b=0.547$  nm and  $c=1.07$  nm tabl.1).

The absence of a distinguishable difference in the breakdown threshold for the two samples is most likely conditioned upon the fact that the LIDT value at the indicated orders of magnitude of the surface roughness parameters is determined not by the quality of polishing, but by the number of point depressions caused by physical limitations of the structural configuration of the crystal volume. These results are in good agreement with the assumption made in [14] about a significant effect of the concentration of dislocations in a ZGP crystal on LIDT. It was noted in [26] that at a sufficiently low concentration, zero-dimensional defects (dislocations, bulk defects), practically without affecting the conditions of radiation propagation due to a weak shadow effect, can significantly reduce the LIDT at the points of their emergence on the surface, playing the role of "nuclei" (or "weak links"), from which the irreversible process of the matrix crystal destruction begins under the action of optical beams of extreme intensity. It can be assumed that the observed point depressions, which are clearly distinguishable during MRP polishing, having dimensions of 0.5–1.5  $\mu\text{m}$ , are a consequence of the "emergence" of dislocations on the surface during the polishing process. As is known, mechanically stressed regions emerge around the dislocations, the presence of which in the process of polishing can cause the appearance of detected point depressions with the above dimensions. An alternative explanation of the results obtained is the presence of volume defects 0.5-1.5  $\mu\text{m}$  in size in the studied ZGP crystals due to the presence of impurities of intrinsic components in the initial synthesized material in the form of binary phosphides of zinc and germanium ( $\text{Zn}_3\text{P}_2$ ,  $\text{ZnP}_2$ ,  $\text{GeP}$ ). These defects could not have been detected during characterization of the samples under study since the resolution of a digital holographic camera used to detect volumetric defects is 3  $\mu\text{m}$ , which is half the size of the detected irregularities. The detective power of X-ray structural analysis may also have turned out to be insufficient. From the above, it can be assumed that one of the possible ways to increase the LIDT is to further improve the technology of synthesis and crystal growth and minimize defects in its structure, as well as improve the characteristics of optical coatings.

## 5. Conclusion

Samples of a single crystal  $\text{ZnGeP}_2$  with an angstrom level of surface roughness have been investigated in this article. Magnetorheological processing was applied to polish the working surfaces of the ZGP single crystal, in which a non-aqueous liquid with magnetic

particles of carbonyl iron with the addition of nanodiamonds was used. The material showed good polishability: MRP led to a significant improvement in surface roughness parameters by 1.37-1.42 times ( $R_a$  1.54Å), as compared to the conventional crystal polishing technique ( $R_a$  2.27Å) using an aqueous suspension based on diamond powder and a resin pad. The removal of material from the crystal surface after MRP ranged from 6.95 to 9.5 μm. Moreover, the use of MRP has allowed more accurately characterizing possible structural defects that have emerged on the surface of a single crystal and have a size of ~ 0.5-1.5 μm. The useful processing time of the 6x6 sample was 8.2% of the total processing time. It is recommended to use the group type of crystal processing during MRP to minimize the time spent on idling and reverse of the working tool, which will significantly increase the efficiency of using industrial equipment. Thus, both polishing methods have allowed obtaining an angstrom level of surface roughness comparable in order of magnitude with the unit cell parameters of the ZGP crystalline lattice, which indicates that the surface quality after MRP is close to the maximum possible.

Despite the fact that the sample subjected to MRP showed a significant improvement in the surface roughness parameters, as compared to the sample polished using the conventional technology, LIDT remained practically unchanged. The absence of a difference in the breakdown threshold for the two samples is most likely conditioned upon the fact that the LIDT value at angstrom parameters of surface roughness is determined to a greater extent not by the quality of polishing, but by the physical limitations of the structural configuration of the crystal. It has been suggested that LIDT was most influenced by dislocations or volume defects "emerging" on the polished surface, rather than by the roughness level. Thus, at the angstrom level of roughness, the decisive factor affecting the LIDT value is the concentration of bulk defects "emerging" on the crystal surface.

**Author Contributions:** Conceptualization, N.Y. and A.K.; methodology, M.Z.; software, G.G.,P.K.; validation, N.Y. and E.S.; formal analysis, O.L.; investigation, N.N.,M.Z., S.P., A.K, G.G.,P.K.; resources, N.Y., A.K.; data curation, E.S.,E.Z.; writing—original draft preparation, E.S.; writing—review and editing, N.Y., S.P.; visualization, M.K.; supervision, N.Y., A.K.; project administration, N.Y., A.K.; funding acquisition, N.Y. All authors have read and agreed to the published version of the manuscript.

**Funding:** This research received no external funding.

**Conflicts of Interest:** The authors declare no conflict of interest. The funders had no role in the design of the study; in the collection, analyses, or interpretation of data; in the writing of the manuscript, or in the decision to publish the results.

## References

1. Yevtushenko A., Rozniakowska-Klosinska M. Encyclopedia of Thermal Stresses. Laser-Induced Thermal Splitting in Homogeneous Body with Coating;. Springer:Berlin, Germany, 2014.
2. Parfenov V.A. Laser materials microprocessing; SPbGETU“LETI”: Saint-Petersburg, Russia, 2011, p.59.
3. Kozub J., Ivanov B., Jayasinghe A., Prasad R., Shen J., Klosner M., Heller D., Mendenhall M., Piston D. W., Joos K., Hutson M. S. Raman-shifted alexandrite laser for soft tissue ablation in the 6- to 7-μm wavelength range. *Biomedical Optics Express* **2011**, 2, pp.1275-1281.
4. Bobrovnikov S.M., Matvienko G.G., Romanovsky O.A., Serikov I.B., Sukhanov A.Ya. Lidar spectroscopic gas analysis of the atmosphere; IOA SB RAS: Tomsk, Russia, 2014. p.510.
5. Romanovskii O.A., Sadovnikov S.A., Kharchenko O.V., Yakovlev S.V. Development of Near/Mid IR differential absorption OPO lidar system for sensing of atmospheric gases. *Optics and Laser Technology* **2019**, 116, pp. 43-47.

6. Bochkovskii D. A., Vasil'eva A. V., Matvienko G., Yakovlev S. V. Application of a strontium vapor laser to laser remote sounding of atmospheric composition. *Atmospheric and Oceanic Optics* **2012**, *25*, pp. 166-170.
7. Schunemann P.G., Zawilski K.T., Pomeranz L.A., Creeden D.J., Budni P.A. Advances in nonlinear optical crystals for mid-infrared coherent sources. *J. Opt. Soc. Am. B* **2016**, *33*, pp.D36-D43.
8. Hemming A., Richards J., Davidson A. A., Carmody N., Bennetts S., Simakov N., Haub J. 99 W mid-IR operation of a ZGP OPO at 25% duty cycle. *Opt. Express* **2013**, *21*, pp. 10062-10069.
9. Haakestad M.W., Fonnum H., Lippert E. Mid-infrared source with 0.2 J pulse energy based on non-linear conversion of Q-switched pulses in ZnGeP<sub>2</sub>. *Opt. Express* **2014**, *22*, pp. 8556-8564.
10. Qian C., Yao B., Zhao B., Liu G., Duan X., Ju Y., Wang Y. High repetition rate 102 W middle infrared ZnGeP<sub>2</sub> master oscillator power amplifier system with thermal lens compensation. *Optics Letters* **2019**, *44*, pp.715-718.
11. Hildenbrand A., Kieleck C., Tyazhev A., Marchev G., Stöppler G., Eichhorn M., Schunemann P. G., Panyutin V. L., Petrov V. Laser damage of the nonlinear crystals CdSiP<sub>2</sub> and ZnGeP<sub>2</sub> studied with nanosecond pulses at 1064 and 2090 nm. *Optical Engineering* **2014**, *53*, p.122511.
12. Gribenyukov A. I., Dyomin V. V., Olshukov A. S., Podzyvalov S. N., Polovcev I.G., Yudin N. N. Investigation of the process of laser-induced damage of ZnGeP<sub>2</sub> crystals using digital holography. *Rus.Phys. J.* **2018**, *61*, pp. 2042–2052.
13. Chumside J.H., Wilson J.J., Gribenyukov A.I., Shubin S.F., Dolgii S.I., Andreev Yu.M., Zuev V.V., Boulder V. in Co:NOAA Technical Memorandum ERL WPL-224 WPL-224 WPL 1992. p.18.
14. Yudin N. N., Antipov O. L., Gribenyukov A. I., Eranov I. D., Podzyvalov S. N., Zinoviev M. M., Voronin L. A., Zhuravleva E. V., Zykova M. P. Effect of postgrowth processing technology and laser radiation parameters at wavelengths of 2091 and 1064 nm on the laser-induced damage threshold in ZnGeP<sub>2</sub> single crystal. *Quantum Electronics* **2021**, *51*, pp.306-316.
15. Andreev Yu. M., Badikov V. V., Voevodin V. G., Geiko L. G., Geiko P. P., Ivashchenko M. V., Karapuzikov A. I., Sherstov I. V. Radiation resistance of nonlinear crystals at a wavelength of 9.55  $\mu\text{m}$ . *Quantum Electronics* **2001**, *31*, pp. 1075-1078.
16. Peterson, R. D., Schepler, K. L., Brown, J. L., Schunemann, P. G. Damage properties of ZnGeP<sub>2</sub> at 2 $\mu\text{m}$ . *J. Opt. Soc. Am. B* **1995**, *12*, pp. 2142-2146.
17. Zawilski K.T., Setzler S.D., Schunemann P.G., Pollak T.M. Increasing the laser-induced damage threshold of single-crystal ZnGeP<sub>2</sub>. *J. Opt. Soc. Am. B* **2006**, *23*, pp. 2310-2316.
18. Lei Z., Zhu C., Xu C., Yao B., Yang C. Growth of crack-free ZnGeP<sub>2</sub> large single crystals for high-power mid-infrared OPO applications. *Journal of Crystal Growth* **2014**, *389*, pp. 23–29.
19. Sutowska M., Sutowski P. Contemporary applications of magnetoreological fluids for finishing process. *Journal of Mechanical and Energy Engineering* **2017**, *1(41)*, pp. 141-152.
20. Verozubova G. A., Gribenyukov A. I., P. Mironov Yu. Two-temperature synthesis of ZnGeP<sub>2</sub>. *Inorganic Materials* **2007**, *43*, pp. 1040–1045.
21. Dyomin V., Gribenyukov A., Davydova A., Zinoviev M., Olshukov A., Podzyvalov S., Polovtsev I., Yudin N., Holography of particles for diagnostics tasks [Invited]. *Appl. Opt.* **2019**, *58*, pp. G300-G310.
22. ISO 11146-1:2005, "Lasers and laser-related equipment - Test methods for laser beam widths, divergence angles and beam propagation ratios".

- 
23. ISO 11146-1:2005, "Lasers and laser-related equipment - Test methods for laser beam widths, divergence angles and beam propagation ratios".
  24. ISO 2602:1980 "Statistical interpretation of test results - Estimation of the mean - Confidence interval".
  25. Fisher R.A., Rothamsted M.A. statistical methods for research workers. *Metron* **1925**, 5, p.90.
  26. Verozubova G.A., Filippov M.M., Gribenyukov A.I., Trofimov A.Yu., Okunev A.O., Stashenko V.A. Investigation of the evolution of structural defects in ZnGeP<sub>2</sub> single crystals, grown by the bridgman method. *Mathematics and mechanics. Physics* **2012**,321. pp. 121-128.